Desalination and Water Treatment
www.deswater.com

doi: 10.5004/dwt.2023.29744

302 (2023) 224–230
August

In-situ growth of manganese oxide/bamboo powder nanocomposites with excellent activity in methylene blue removal

Guanhui Wang[a], Wenxiang Li[a], Hanli Wang[b], Congcong Bi[b], Runlin Han[a,b,*]

[a]*School of Chemistry and Chemical Engineering, Jinggangshan University, Ji'an 343009, China, emails: hanrunlin@163.com (R. Han), wangguanhui@jgsu.edu.cn (G. Wang), 2383639321@qq.com (W. Li)*
[b]*Shandong Huaxia Shenzhou New Material Co., Ltd., Zibo 256400, China, emails: whl89333@huaxiashenzhou.com (H. Wang), szzscq@huaxiashenzhou.com (C. Bi)*

Received 16 March 2023; Accepted 30 June 2023

ABSTRACT

Cellulose is rich in sources and contains a large number of hydroxyl groups in the molecule, which can be used as the carrier of nanomaterials and reducing agents of $KMnO_4$. Manganese oxide (MnO_2)/bamboo powder nanocomposites were prepared at 60°C using wood powder as a reducing agent and nanomaterials carrier. $KMnO_4$ was utilized as an oxidant and manganese source of MnO_2 nanoparticles. Methylene blue was used as the target pollutant to test the activity of nanocomposites. Under neutral conditions, the removal efficiency of methylene blue reached 98.5% under room temperature and atmospheric pressure, and the maximum adsorption capacity of the nanocomposite reached in 10 min.

Keywords: Wood powder; Manganese oxide; Composite material; Methylene blue; Wastewater treatment

1. Introduction

There is an urgent need for efficient and sustainable technologies to solve environmental problems. Many technologies have been used to treat dye wastewater, among which nano-catalyst technology is considered to be one of the most effective technology solutions. Currently, there are many kinds of nano-catalysts used for environmental purification, including precious metals, metal sulfides, metal carbides, metal oxides, and other carbon-based materials such as GO, molecular sieves, graphitic carbon nitride (g-C_3N_4) based composites etc [1–3]. Moreover, the g-C_3N_4 nanosheets were new modified two-dimensional graphene-like nanomaterials which showed high potential in organic pollutants degradation because of high photocatalytic activity [4]. Considering the abundance, cost, toxicity, environmental adaptability, and purification activity of the material, nano MnO_x was widely used for environmental purification. Moreover, it is an excellent nano-catalyst material with variable valence, strong oxidation ability, and high adsorption capacity, which can realize the efficient treatment of organic wastewater [5]. Our group has prepared nanosized Mn_3O_4 nanowires with $KMnO_4$ and ethanol in mild conditions by facile hydrothermal method. The nanowires exhibited high activity in the treatment of dye and phenol at the acid condition and room temperature. $KMnO_4$ was used as an oxidant and ethanol was used as a reducing agent [6,7].

When nanomaterials are used for organic wastewater treatment, particles agglomeration, and catalytic deactivation are likely to occur. To improve catalyst efficiency, nanomaterials can be compounded on appropriate carriers [8]. Cellulose fibers are considered a suitable carrier because cellulose is a renewable, widely sourced raw material with a relatively large surface area, low density, and environmental friendliness. Wang et al. [9] proposed an efficient synthesis method for MnO_2/cellulose composites. Bamboo cellulose is not only

* Corresponding author.

a reducing agent but also an ultralight carrier for the synthesis of MnO_2/cellulose composite. The composite has both oxidation and adsorption effects, and the results show that the removal rate of methylene blue within 2 min is greater than 99.8%. However, the composite requires a certain amount of NaOH in the synthesis process, and the preparation process of cellulose used is slightly complicated. Gupta et al. [10] prepared MnO_2/cellulose composites by microwave-assisted hydrothermal synthesis. The specific surface area of the composite is 87.064 m^2/g, and the particle size of the nanoparticles is about 70 nm. The composite has a high treatment efficiency for the pesticide octachor camphene, with removal of 96.5% at pH 3. Bamboo is known to have a very short growth cycle and contains a lot of cellulose. It can reduce the costs of nanocomposites and filtration systems greatly which is a excellent candidate of composite carrier [11,12].

In this work, the natural bamboo powder was used as a reducing agent and composite carrier. $KMnO_4$ was used as an oxidation reagent and manganese source. No other chemical reagents were used which achieved the green synthesis of MnO_2/cellulose nanocomposites. The effects of $KMnO_4$ dosage, hydrothermal reaction time, and other factors on the properties of composite materials are investigated. Using methylene blue as target pollution, the reaction time and other effects on dye treatment efficiency were investigated in detail.

2. Experimental set-up

2.1. Materials

The bamboo powder was provided by Suichuan Huimin Wood and Bamboo Processing Plant (Jiangxi Province, China). $KMnO_4$ was purchased from Sinopharm Chemical Reagent Co., Ltd., (Shanghai, China). Methylene blue and other dyes are provided by Tianjin Zhiyuan Chemical reagent Co., Ltd., (Tianjin, China).

2.2. Nanomaterials preparation

A certain amount of $KMnO_4$ was added into a 50 mL flask and 30 mL deionized water was added to dissolve it for later use. 0.5 g of bamboo powder was added into the solution with strong agitation at 60°C for 1 h. After reaction, the mixture was washed with deionized water, and the nanocomposites were dried in the oven at 80°C. The dried powder was ground for use.

2.3. Nanomaterials characterization

100 mL methylene blue solution with a concentration of 100 mg/L was used as the target pollutant. 0.1 g nanocomposite material was added in the dye solution, and stirred for 15 min at room temperature and pressure. After the stirring was completed, the absorbance of the dye solution before and after treatment was measured by UV-Vis spectrometer (721, Shanghai Youke, China) at the maximum absorption wavelength of dye, and the removal efficiency of the dye before and after the sample added was calculated. For the cycle stability test of nanocomposites, the nanomaterials after dye adsorption were filtered and washed with ethanol. Then they were reused after dried in the oven.

The removal efficiency was calculated as follows:

$$R = 100\left(1 - \frac{C_i}{C_f}\right)\%$$

where c_i and c_f are the initial and final (equilibrium) concentrations of the dye in the solution (mg/L), respectively.

All the experiments on flux and rejection were repeated for three times. The relation standard deviation of the data was lower than 15%. The material morphology was tested with scanning electron microscopy (SEM, NanoSEM 450, FEI, USA) equipped with INCA energy-dispersive X-ray spectroscopy (EDX). The element composition was tested with X-ray photoelectron spectroscopy (XPS, Thermo ESCALAB 250Xi, USA). The samples were tested with the specific surface area aperture (Quantachrome ASAP 2460, USA) to investigate their structural properties and porous parameters via the N_2 adsorption and desorption test at 77 K. X-ray powder diffraction (XRD, Rigaku SmartLab SE, Japan) was measured to determine the crystal structure of the samples using Cu Kα radiation at 40 kV and 30 mA.

3. Results and discussion

3.1. Characterization of the nanomaterials

To explore the relationship between the structure and properties of nanocomposites, SEM was used to characterize the morphologies of the nanocomposites. When the content of $KMnO_4$ was 0.2 g as shown in Fig. 1, the nanosized manganese oxide nanoparticles in the composites are little. When the content of $KMnO_4$ increased to 0.4 g, the nano-sized MnO_2 content in the nanocomposites increased a lot, which also increases the specific surface area of the nanocomposites. The morphology of bamboo powder is also presented in Fig. 1. The surface of the powder was very smooth with some fiber.

The element composition of the nanocomposite was analyzed by surface scanning with EDX. It can be seen from Fig. 2 that the material is mainly composed of C, O, and N elements without other impurities. Element C is mainly derived from bamboo fibers, while Mn is derived from manganese oxide produced by the reduction of $KMnO_4$. It can also be seen from the figure that the distribution of the Mn element in the material is very uniform. As shown in Table 1, the C content was the highest, which is due to the use of bamboo powder as a reducing agent, which contains a large amount of bamboo fiber, hemicellulose, and lignin. There was also a large amount of the Mn element in the nanocomposites, because of the reduction of $KMnO_4$ by the hydroxyl group in the cellulose fiber. The formed MnO_2 will not be dissolved by water and successfully composited on the fiber.

The nanomaterial prepared with 0.4 g $KMnO_4$ was tested with XPS. Fig. 3 shows the electron region of the XPS spectra of the nanocomposite and high-resolution spectra of Mn 2p. The sharp peak at 282 eV was attributable to C 1s, which generated from the bamboo powder. The peak at 532 eV corresponded to O 1s which generated from MnO_x and the bamboo powder. The peaks located at 641.9 and 653.8 eV were attributable to Mn $2p_{3/2}$ and Mn

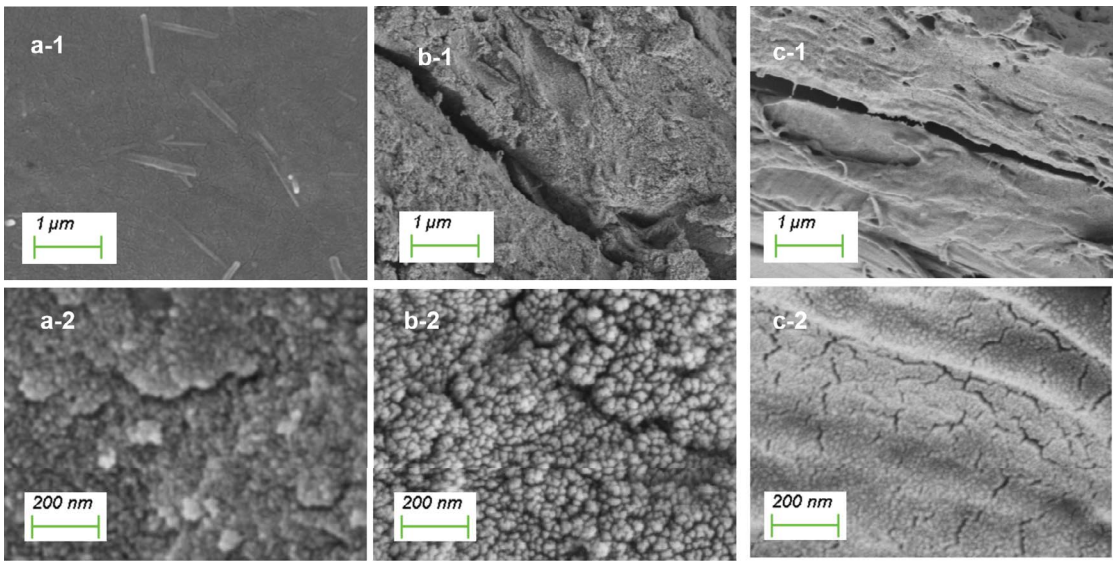

Fig. 1. Morphology of nanocomposites. (a) 0.2 g $KMnO_4$, (b) 0.4 g $KMnO_4$, (c) bamboo powder.

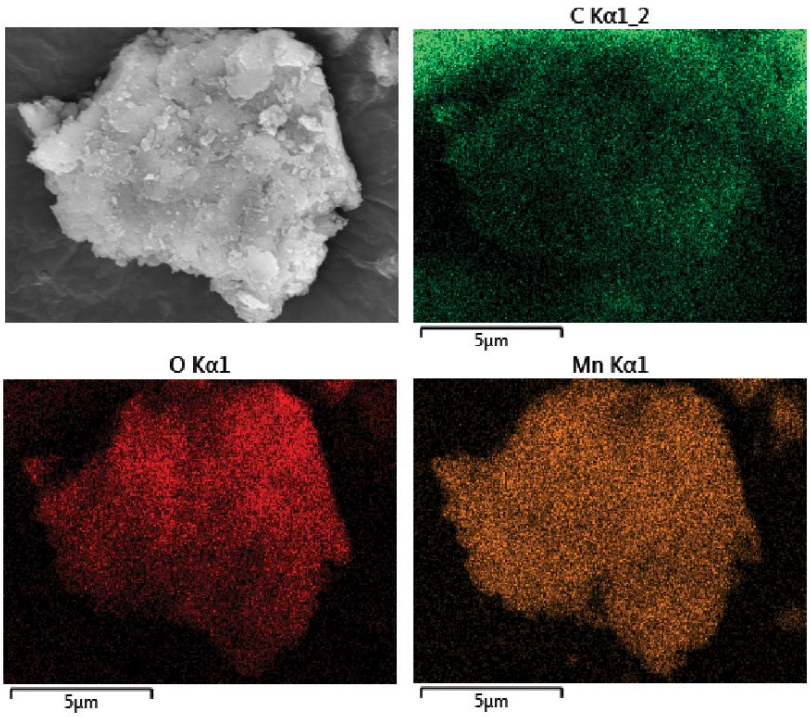

Fig. 2. Energy-dispersive X-ray spectroscopy of the nanocomposites (prepared with 0.4 g $KMnO_4$).

$2p_{1/2}$, respectively. The Mn 2p XPS spectrum suggested that Mn was present in its IV state, and the nanosized MnO_2 was formed during the hydrothermal reaction. According to Fig. 3c, the high-resolution C 1s XPS spectra show the peaks including C=C (284.4 eV), C–O (286 eV), and COO (288 eV). The high-resolution O 1s spectrum of the composite nanomaterials shown in Fig. 3d demonstrates the C=O (530.8 eV), COO– (532.7 eV), CO (530.8 eV) and O–Mn (529.5 eV) configurations [13].

The Fourier-transform infrared spectra of nanocomposites and bamboo powder are shown in Fig. 4. Both spectra revealed the characteristic absorption peaks of cellulose. The peak located at 3,300 cm^{-1} was attributed to O–H stretching of cellulose. The peak at 1,050 cm^{-1} was assigned to the C–O stretching in cellulose. Especially, the enhanced peak at around 1,590 cm^{-1} of nanocomposites was caused by the C=O group because of –OH of the cellulose was oxidized by $KMnO_4$.

The XRD patterns of the nanocomposites and bamboo powder are shown in Fig. 5. The diffraction peak of bamboo powder at about 23° was attributed to disordered carbonaceous structure (the crystallographic plane of 002) [14]. The disappearance of the peak of nanocomposites demonstrated that the addition of MnO_2 might restrain the formation of crystal structure. As can be seen from the figure, the diffraction peaks of the two samples are not strong, because the main component of the materials are cellulose, which has low crystallinity.

Table 1
Element composition of the nanocomposites prepared with 0.4 g $KMnO_4$

Elements	Weight (%)	Atom (%)
Mn	44.55	16.32
O	22.06	27.75
C	33.38	55.93

The textural parameters of the bamboo powder and nanocomposites are listed in Table 2. The bamboo powder without modification showed very low Brunauer–Emmett–Teller (BET) surface area (0.53 m^2/g) and pore volume (0.0084 cm^3/g). The nanocomposites showed higher BET surface area (27.33 m^2/g) and pore volume (0.048 cm^3/g) because of introduction of nanosized MnO_2. The result was consistent with SEM images. The average pore diameter of nanocomposites was a little higher maybe caused by the pore structure of MnO_2 nanoparticles on the cellulose carrier.

3.2. Performance of the nanocomposites

The effect of $KMnO_4$ content on properties of nanocomposites was investigated with methylene blue used as the target pollutant. Methylene blue solution with a concentration of 100 mg/L was taken as the target pollutant and treated with the bamboo powder or nanocomposites for 15 min at room temperature and atmospheric pressure. Bamboo powder without modification was also used to treat the dye solution as a control experiment. As can be seen from Fig. 6, the

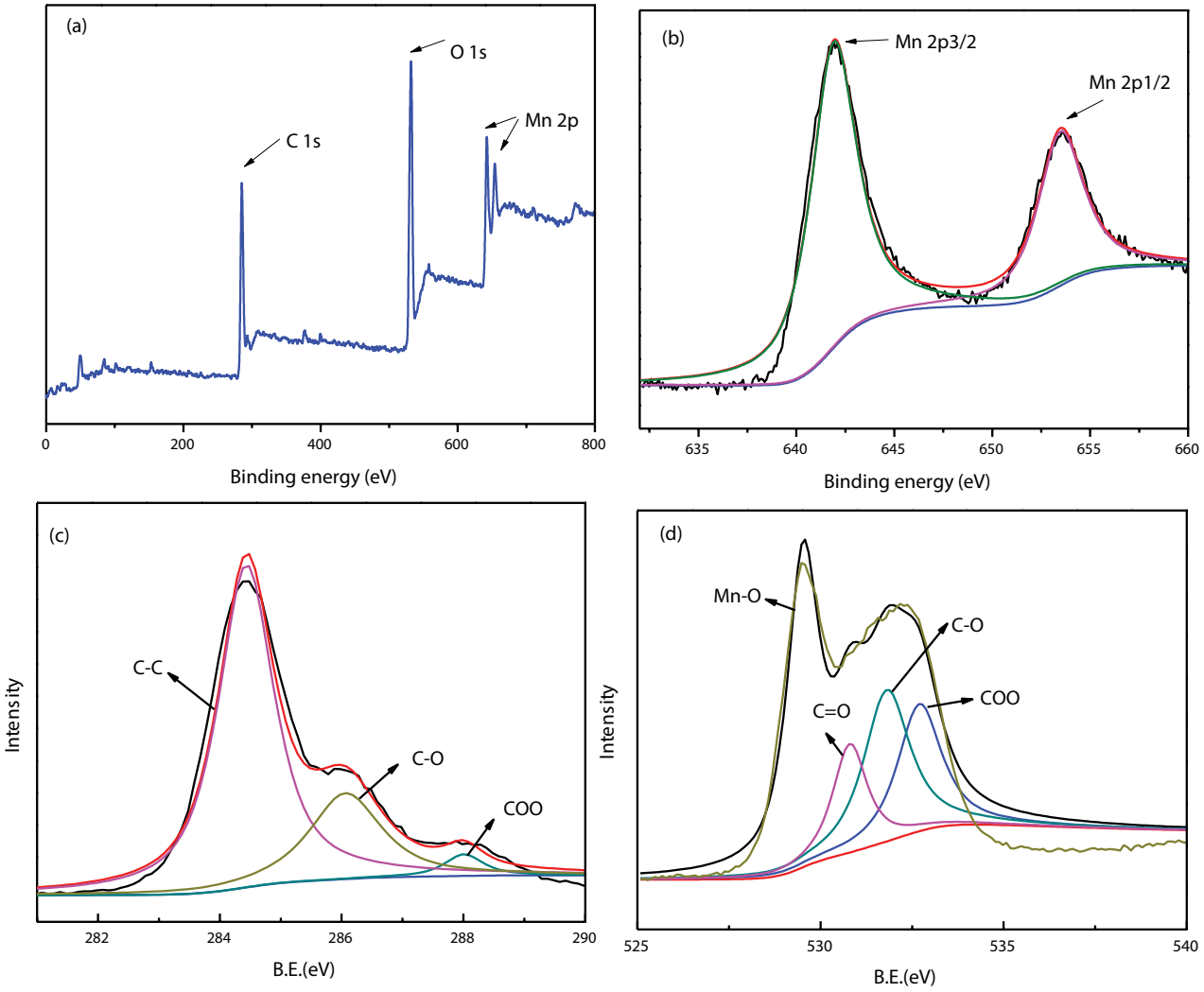

Fig. 3. X-ray photoelectron spectra of nanocomposites. (a) Survey spectrum, (b) detailed spectrum of Mn 2p, (c) detailed spectrum of C 1s, and (d) detailed spectrum of O 1s.

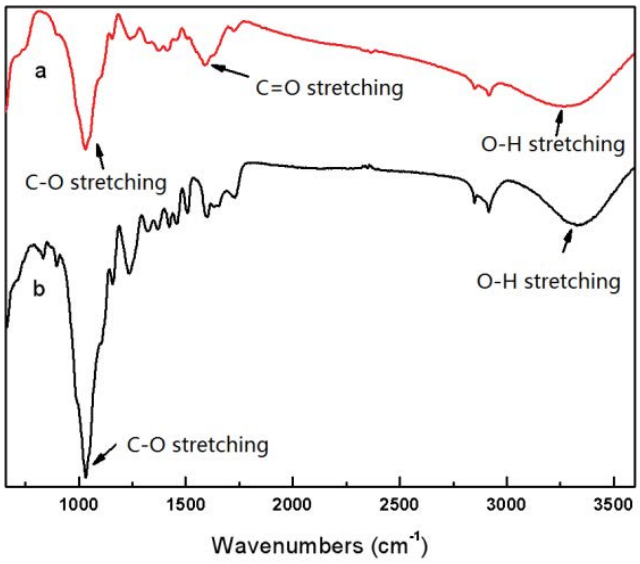

Fig. 4. Fourier-transform infrared spectra of the nanocomposites (a) and bamboo powder (b).

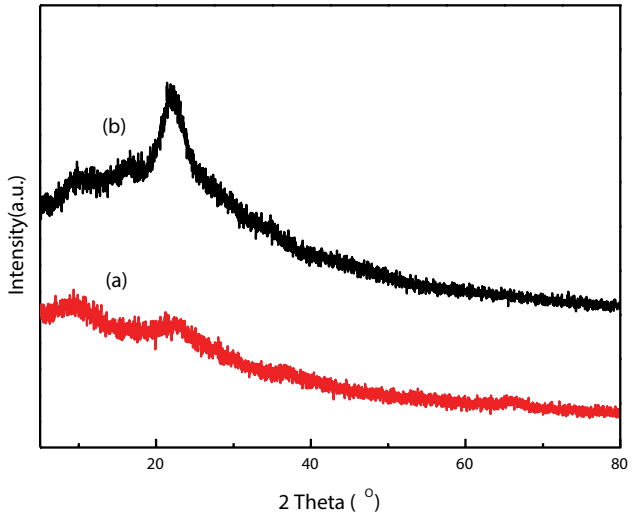

Fig. 5. X-ray powder diffraction patterns of the nanocomposites (a) and bamboo powder (b).

Table 2
N_2 physical adsorption data of samples

Sample	S_{BET} (m^2/g)	Pore volume (cm^3/g)	Pore diameter (nm)
Bamboo powder	0.53	0.0084	6.37
Nanocomposites	27.33	0.048	6.97

removal rate of bamboo powder can reach 59.2%, because bamboo powder also has a strong adsorption capacity. The weight of cellulose powder was fixed to 0.5 g, and the $KMnO_4$ content was increased from 0.1 to 0.7 g to prepare nanocomposites. The reaction temperature was fixed at 60°C

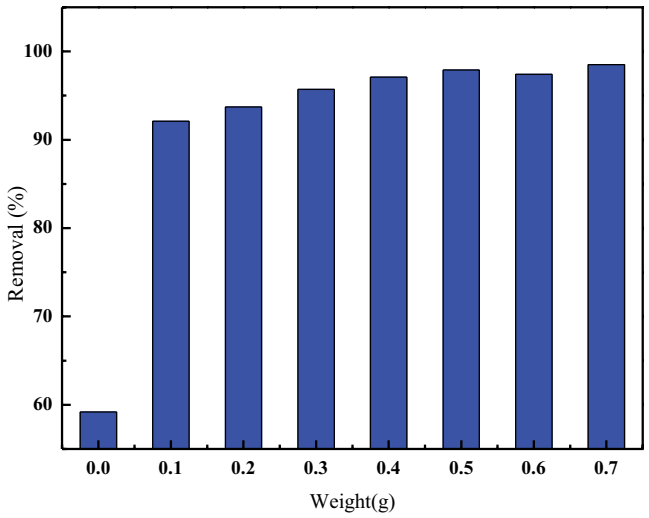

Fig. 6. Effect of $KMnO_4$ content on the properties of nanocomposites.

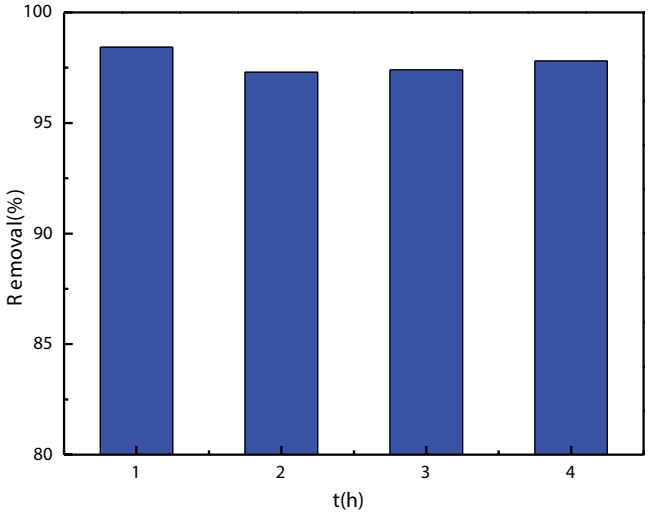

Fig. 7. Effect of hydrothermal reaction time on the activity of the nanocomposites.

for 1 h, and the products were obtained by filtering, drying and grinding. As shown in Fig. 6, the content of $KMnO_4$ has a great influence on the treatment performance of the nanocomposites. When the content of $KMnO_4$ was above 0.4 g, the removal rate of dye solution was above 97%. When the content of $KMnO_4$ was 0.7 g, the removal rate of methylene blue dye was 98.5%. The –OH group on the surface of the fibers reacted with $KMnO_4$. Due to the high crystallinity of cellulose, $KMnO_4$ is difficult to penetrate the crystals. More $KMnO_4$ has less effect on the performance. So, the content of $KMnO_4$ was determined to be 0.4 g in the subsequent study.

The effect of reaction time on the properties of the nanocomposites was investigated when the reaction temperature was 60°C and the amount of $KMnO_4$ was 0.4 g as shown in Fig. 7. 100 mL methylene blue solution (100 mg/L) was treated for 15 min to explore the treatment properties of

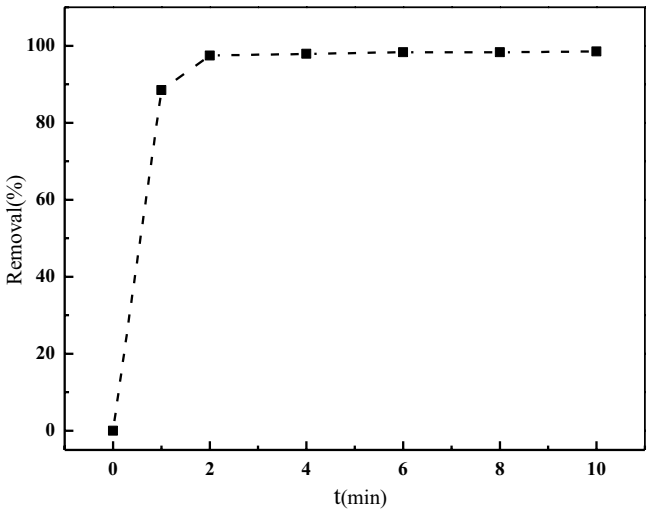

Fig. 8. Effect of adsorption time on the dye removal.

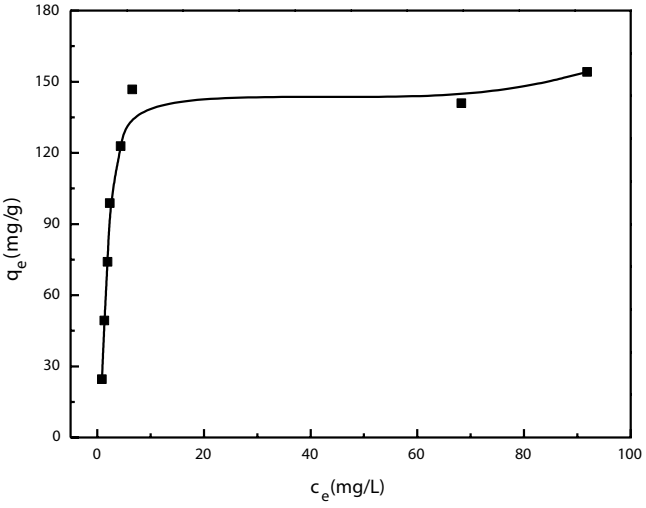

Fig. 9. Adsorption isotherm of the nanocomposites.

composite dyes under different hydrothermal reaction times. It can be seen from Fig. 7 that the removal rates of methylene blue under different reaction times are all above 97%, indicating a high treatment efficiency. The reaction time of 1 h is effective for the preparation of nanomaterials with good performance. Therefore, the subsequent preparation time of nanocomposite was fixed at 1 h.

To determine the treatment efficiency of the nanocomposites, 0.1 g of the sample was added into the solution with different adsorption times. The dye removal rate is shown in Fig. 8. It can be seen from the figure that when the composite material was added into the dye solution for 1 min, the removal rate of methylene blue reached 88.5%, which reached a high removal rate in a very short time. When the adsorption time was extended to 2 min, the dye removal efficiency reached 97.4%. With the extension of time, the processing rate is further improved but slowly. After 10 min of processing, the dye treatment rate reached 98.5%. The results showed that the nanocomposites had high activity at room temperature and atmospheric pressure.

The adsorption data onto nanocomposites were analyzed to investigate the relationship between adsorbent and dye in solution as shown in Fig. 9. When the initial concentrations of methylene blue increased from 50 to 200 mg/L, the amount of equilibrium absorption grew steeply with the increase of equilibrium concentration of dye solution. When the initial concentration was above 250 mg/L, the amount of equilibrium absorption changed little. The maximum adsorption capacity reached up to 154 mg/g when the initial concentration was 400 mg/L.

To investigate the cyclic stability of nanocomposites, the nanomaterial after treatment of methylene blue solution were filtered, dried, and recycled. Then the recycled materials were used to treat dye solution under the same conditions. Fig. 10 shows the performance of nanomaterial during four cycles. As can be seen from the figure, the nanomaterials exhibited very good cyclic stability in the treatment of dye wastewater. After four cycles, the dye removal rate of the material was still above 86.4%. The results showed that the chemical stability of the nanocomposites was very

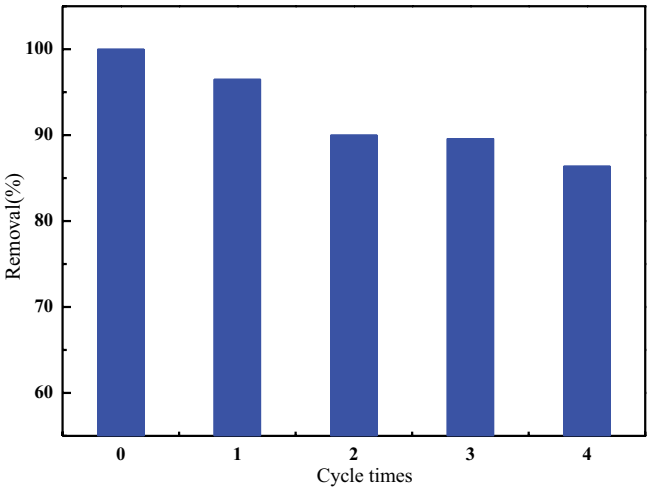

Fig. 10. Effect of cycle times on the dye removal.

high. The MnO_2 nanoparticles contained in the sample have certain catalytic activity. It can catalyze the dye molecules adsorbed on the surface of the material, thus maintaining high processing efficiency. At the same time, nanoparticles and cellulose carriers combined closely. So, the nanoparticles were not easy to lose during utilization and filtration.

4. Conclusions

In conclusion, MnO_2/bamboo powder nanocomposites were prepared by hydrothermal reaction. Cellulose was used as a reducing agent and carrier while $KMnO_4$ was used as the manganese source and oxidant. The morphology and composition of the materials were analyzed by SEM and XPS. The results showed that the nanocomposites with typical MnO_2 nano spheres can be prepared by using bamboo powder as the reducing agent and nanoparticles carrier under mild hydrothermal conditions. The distribution of MnO_2 nanoparticles is relatively uniform according to EDX mapping. The nanocomposites showed higher BET surface

area which improved the dye removal activity. The preparation condition was green without using any other chemicals. The synthesis reaction condition was relatively mild. The required reaction temperature was 60°C and the reaction time was 1 h. When the $KMnO_4$ content was 0.4 g, the dye treatment efficiency of the prepared nanocomposites can reach more than 98.5% under neutral and room temperature conditions. The nanomaterials also have good cycling stability, because the dye treatment efficiency of the material can still reach more than 86.4% after four cycles.

Acknowledgements

This research was funded by Jiangxi Province Double Thousand Talents Plan, grant number jxsq2020101049; Science & Technology Program of Jiangxi Provincial Education Bureau, grant number GJJ2201623, GJJ190573; China Postdoctoral Science Foundation, grant number 2021M691964.

Conflicts of interest

The authors declare no conflict of interest.

References

[1] N.Y. Donkadokula, A.K. Kola, I. Naz, D. Saroj, A review on advanced physico-chemical and biological textile dye wastewater treatment techniques, Rev. Environ. Sci. Bio/Technol., 19 (2020) 543–560.
[2] K. Sharma, S. Sharma, V. Sharma, P.K. Mishra, A. Ekielski, V. Sharma, V. Kumar, Methylene blue dye adsorption from wastewater using hydroxyapatite/gold nanocomposite: kinetic and thermodynamics studies, Nanomaterials, 11 (2021) 1403, doi: 10.3390/nano11061403.
[3] Y. Chen, A. Li, X. Fu, Z. Peng, Novel F-doped carbon nanotube@(N,F)-co-doped $TiO_{2-\delta}$ nanocomposite: highly active visible-light-driven photocatalysts for water decontamination, Appl. Surf. Sci., 609 (2023) 155460, doi: 10.1016/j.apsusc.2022.155460.
[4] R. Yang, Y. Fan, R. Ye, Y. Tang, X. Cao, Z. Yin, Z. Zeng, MnO_2-based materials for environmental applications, Adv. Mater., 33 (2021) 2004862, doi: 10.1002/adma.202004862.
[5] A. Akhundi, A. Badiei, G.M. Ziarani, A. Habibi-Yangjeh, M.J. Muñoz-Batista, R. Luque, Graphitic carbon nitride-based photocatalysts: toward efficient organic transformation for value-added chemicals production, Mol. Catal., 488 (2020) 110902, doi: 10.1016/j.mcat.2020.110902.
[6] R. Han, Y. Zhang, Y. Xie, Application of Mn_3O_4 nanowires in the dye wastewater treatment at room temperature, Sep. Purif. Technol., 234 (2020) 116119, doi: 10.1016/j.seppur.2019.116119.
[7] R. Han, M. Chen, X. Liu, Y. Zhang, Y. Xie, Y. Sui, Controllable synthesis of Mn_3O_4 nanowires and application in the treatment of phenol at room temperature, Nanomaterials, 10 (2020) 461, doi: 10.3390/nano10030461.
[8] S. Xu, J. Yang, J. Li, F. Shen, Highly efficient oxidation of biomass xylose to formic acid with CeO_x-promoted MnO_x catalyst in water, ACS Sustainable Chem. Eng., 11 (2023) 921–930.
[9] Y. Wang, X. Zhang, X. He, W. Zhang, X. Zhang, C. Lu, *In-situ* synthesis of MnO_2 coated cellulose nanofibers hybrid for effective removal of methylene blue, Carbohydr. Polym., 110 (2014) 302–308.
[10] V.K. Gupta, A. Fakhri, S. Agarwal, N. Sadeghi, Synthesis of MnO_2/cellulose fiber nanocomposites for rapid adsorption of insecticide compound and optimization by response surface methodology, Int. J. Biol. Macromol., 102 (2017) 840–846.
[11] D. Wang, A critical review of cellulose-based nanomaterials for water purification in industrial processes, Cellulose, 26 (2019) 687–701.
[12] R.E. Abouzeid, R. Khiari, N. El-Wakil, A. Dufresne, Current state and new trends in the use of cellulose nanomaterials for wastewater treatment, Biomacromolecules, 20 (2019) 573–597.
[13] J. Xiao, N. Xiao, K. Li, L. Zhang, X. Ma, Y. Li, C. Leng, J. Qiu, Sodium metal anodes with self-correction function based on fluorine-superdoped CNTs/cellulose nanofibrils composite paper, Adv. Funct. Mater., 32 (2022) 2111133, doi: 10.1002/adfm.202111133.
[14] Z. Dai, P. Ren, Q. Cao, X. Gao, W. He, Y. Xiao, Y. Jin, F. Ren, Synthesis of TiO_2@lignin-based carbon nanofibers composite materials with highly efficient photocatalytic to methylene blue dye, J. Polym. Res., 27 (2020) 108, doi: 10.1007/s10965-020-02068-7.